

T-CAD analysis of electric fields in n-in-p silicon strip detectors in dependence on the p-stop pattern and doping concentration

This content has been downloaded from IOPscience. Please scroll down to see the full text.

2015 JINST 10 C01048

(<http://iopscience.iop.org/1748-0221/10/01/C01048>)

View [the table of contents for this issue](#), or go to the [journal homepage](#) for more

Download details:

IP Address: 146.137.70.71

This content was downloaded on 16/06/2015 at 22:24

Please note that [terms and conditions apply](#).

10th INTERNATIONAL CONFERENCE ON POSITION SENSITIVE DETECTORS
7–12 SEPTEMBER 2014,
UNIVERSITY OF SURREY, GUILDFORD, SURREY, U.K.

T-CAD analysis of electric fields in n-in-p silicon strip detectors in dependence on the p-stop pattern and doping concentration

M. Printz on behalf of CMS Tracker collaboration

*Institut fuer Experimentelle Kernphysik,
Wolfgang-Gaede-Str. 1, 76131 Karlsruhe, Germany*

E-mail: martin.printz@kit.edu

2015 JINST 10 C01048

ABSTRACT: Detectors based on silicon have been proven to be efficient for particle tracking in high energy physics collider experiments. The Compact Muon Solenoid (CMS) Tracker at CERN near Geneva has a silicon detector surface of about 200 m². The increasing demand on more collected data for new physics studies requires an upgrade of the Large Hadron Collider to higher luminosity which is foreseen for 2023. The increase of particles per time and area also introduces a harsh environment for the silicon sensors which should withstand an integrated luminosity of about $L = 3000 \text{ fb}^{-1}$. Several R&D studies have been undertaken to face the high luminosity challenge and n-in-p detectors have been found to be more radiation hard than p-in-n.

However, n-in-p detectors necessarily need an isolation layer of the n+ strips due to an accumulation layer of electrons caused by positive charge in the SiO₂ at the sensor surface. An additional implantation of acceptors like boron between the n+ strips cuts the conducting electron layer and ensures reliable strip isolation. However, the implantation dose as well as the implant energy have to be carefully calculated as they directly affect the breakdown behavior and inter-strip resistance of the sensors.

Experimentally, the inter-strip resistance (R_{int}) and charge collection efficiency (CCE) as well as the cluster charge formation are a direct indicator whether the isolation layer is sufficient or not. Furthermore T-CAD simulation studies have been carried out in order to reproduce the measurements and to predict the performance of sensors before and after irradiation with protons, neutrons and a mixture of both. Simulations also allow detailed studies of the formation of electric fields in the sensor which influence the sensor performance. Experimentally obtained CCE and misidentified hits in n-in-p devices with p-stop isolation pattern can be explained after analysis of the electric fields in dependence on the p-stop geometry and doping concentrations.

The comparison of data and simulation results allows to limit the parameter space of the p-stop isolation technique which significantly affects the performance of irradiated n-in-p type silicon sensors.

KEYWORDS: Particle tracking detectors; Si microstrip and pad detectors; Radiation-hard detectors; Particle detectors

Contents

1	LHC and CMS upgrade	1
2	Development of n-in-p type sensors	1
3	T-CAD studies on p-stop parameters	2
3.1	Electric fields and charge collection before irradiation	3
3.2	Electric fields and charge collection after irradiation	4
4	Conclusions and outlook	6

1 LHC and CMS upgrade

The analysis of physics data collected by experiments at the Large Hadron Collider and studies of physics beyond the standard model requires an increase of the luminosity for more statistics. Therefore a machine upgrade is foreseen for 2023 when the high luminosity (HL) era of the LHC will start. The experiments at HL-LHC will face an integrated luminosity of about 3000 fb^{-1} after 10 years of operation. Hence, the experiments will be exposed to a higher radiation environment and need to be upgraded, too. Significant changes in the CMS tracker geometry as well as the sensor material used must be carried out in order to cope with the increased number of penetrating particles. The CMS tracker will be replaced completely. The new tracker will be equipped with n-in-p type sensors as several R&D studies showed an enhanced radiation hardness of this sensor type [1–3].

The expected fluence in CMS for the inner layers of the Tracker ($R \sim 20 \text{ cm}$) which will be equipped with silicon strip sensors is about $F = 1 \times 10^{15} \text{ n}_{\text{eq}} \text{ cm}^{-2}$. This high fluence introduces significant bulk and oxide damage in sensors and therefore studies on radiation hard material and geometry as well as process parameters and isolation techniques of n-in-p type sensors are fundamental.

2 Development of n-in-p type sensors

Silicon sensors are passivated with SiO_2 which is positively charged due to technological processes. Even before irradiation, the positive oxide charge can reach values of about 10^{11} cm^{-2} . Furthermore, the oxide charge increases after irradiation with charged particles up to $3 \times 10^{12} \text{ cm}^{-2}$ depending on the oxide thickness and crystal orientation [4]. Hence, electrons are accumulated due to this positive charge at the Si/ SiO_2 interface of n-in-p type detectors. Accordingly the n+ implants can be shorted and the generated signal would spread over several strips. As a consequence some hits would not be identified because the resulting signal could be less than 5 times sigma of the

Table 1. Parameters of the samples from different vendors. These values have been taken as parameter input for the following T-CAD simulation studies.

Sample #	p-stop peak conc. (cm^{-3})	p-stop depth (μm)	Pitch (μm)	Thickness (μm)
1	$\ll 1 \times 10^{16}$	~ 1.5	90	290
2	$\sim 1 \times 10^{16}$	~ 2.0	80	300
3	$\sim 9 \times 10^{16}$	~ 2.7	90	270

gaussian noise what is the definition for a hit. Furthermore, the signal to noise ratio (SNR) would decrease significantly.

In order to insulate the implant from the accumulation layer, a uniform p+ layer (p-spray) can be doped between the strips or certain p+ patterns (p-stop) can be realized at the cost of an additional mask. The latter is a promising technology for the CMS Tracker Upgrade since it is difficult to meet the p-spray dose for sufficient strip isolation but simultaneously reach high breakdown voltages [5]. On the other hand, the pattern of the p-stop as well as doping concentration and depth are crucial too, for good sensor performance after high irradiation.

Float-zone samples from three different vendors with different doping concentrations but comparable strip design have been measured and accompanying Synopsys T-CAD simulation studies have been carried out. The pitch of the samples was either $80 \mu\text{m}$ or $90 \mu\text{m}$ with a width to pitch ratio of $w/p = 0.22$. The p-stops are $6 \mu\text{m}$ wide and implanted about $25 \mu\text{m}$ next to the n+ strip. This means that each strip is surrounded by an individual p-stop ring [6] what is defined as the p-stop atoll configuration. The sensors mainly vary in the bulk thickness and the p-stop concentration and doping depth. The values are listed in table 1.

The parameters of samples #2 are known from SIMS¹ measurements and the parameters of samples #1 and #3 have been communicated by the vendors. All simulations have been carried out with these values as input parameters in order to receive reliable results.

3 T-CAD studies on p-stop parameters

T-CAD simulations can be a suitable and cost reducing tool for silicon sensor development. Within the CMS Upgrade sensors R&D, several radiation damage models have been developed using data from measurements. While the leakage current increases after irradiation, the charge collection efficiency (CCE) decreases steadily due to trapping of the charges moving to the readout electrodes. Therefore simulations are carried out to investigate the formation of electric fields and charge collection after the expected particle fluence of the future CMS detector. The damage model presented in table 2 was developed by R. Eber in [7] considering the current and capacitance over voltage characteristics as well as TCT² and CCE measurements.

This model was chosen for simulations of irradiated devices in this work. For comparability with measurements, the simulations of irradiated devices have been performed at $T = 253 \text{ K}$.

¹Secondary Ion Mass Spectroscopy.

²Transient Current Technique.

Table 2. Effective two defect damage model for proton irradiation of silicon sensors for $T = 253$ K [7]. E_C and E_V are the edge energies of the conduction and valence band. σ_e and σ_h are the cross sections for electrons and holes. Φ is the fluence.

Defect	Energy (eV)	σ_e (cm ⁻²)	σ_h (cm ⁻²)	Concentration (cm ⁻³)
Acceptor	$E_C - 0.525$	1.2×10^{-14}	1.2×10^{-14}	$1.55 \times \Phi$
Donor	$E_V + 0.48$	1.2×10^{-14}	1.2×10^{-14}	$1.395 \times \Phi$

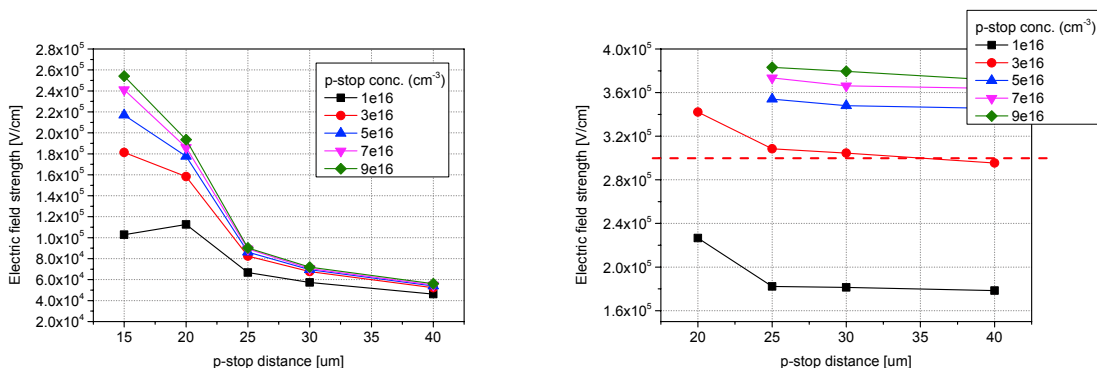
3.1 Electric fields and charge collection before irradiation

Simulations of unirradiated devices without any damage models applied are able to reproduce sensor performance quite accurately. Within this study, the maximum electric fields, which occur in the silicon bulk, have been evaluated before irradiation and after proton irradiation by applying the damage model. For this purpose, the geometry parameters have been taken from the GDS files of the masks for production. Doping concentrations and depth which have been chosen are presented in table 1. The oxide charge has been realized in the simulations as a density of positively charged interface defects N_{Ox} at the interface of silicon and SiO_2 .

Variations of the distance between the n+ strip and p-stop implants have been performed and the maximum electric field in the silicon independent of the position where it occurs has been extracted. Figure 1(a) shows that the electric fields decrease with increasing distance. **In the unirradiated case, simulations have been performed at $T = 293$ K and $V_{Bias} = -300$ V while N_{Ox} has been kept constant to 1×10^{11} cm⁻².** Hence, the pattern of the p-stop atoll configuration could significantly influence the performance of the sensors due to the dependence of the electric fields. Especially, when the maximum electric field strength exceeds $\sim 3 \times 10^5$ V/cm as this is the electrical breakdown voltage of silicon. As a consequence, p-stops should be preferably implanted in the center of two adjacent n+ strips because in this case the maximum electric fields in the bulk are lowest and the breakdown behavior improves.

Signal measurements have been performed with the ALiBaVa³ System [9] based on the analogue Beetle chip used in the LHCb experiment. Penetrating electrons from the β^- decay of a Sr^{90} source have been triggered by a scintillator and measurements have been performed before and after mixed irradiation up to a fluence of 1.5×10^{15} n_{eq} cm⁻² ($R = 20$ cm). At this radial distance from the interaction point, modules equipped with silicon strip sensors will be mounted during the HL-LHC era. From the batch of samples#3, where two different p-stop distances ($16 \mu\text{m}$ and $25 \mu\text{m}$) have been produced, no difference in charge collection in dependence on the p-stop distance to n+ strips has been observed. For the T-CAD studies a minimal ionising particle (MIP) was used with a charge per unit length of $80e^-/h$. After simulation of a $300 \mu\text{m}$ thick device, the arithmetic mean charge of $25807e^-$ with a root mean square of $\sigma = 799e^-$ which corresponds to about $86e^-/\mu\text{m}$ was generated. This is in agreement with the generated charge in $300 \mu\text{m}$ of silicon which is about $80e^-/h$ pairs per μm .

³A Liverpool Barcelona Valencia.



(a) unirradiated; $V_{\text{bias}} = -300\text{V}$; $N_{\text{Ox}} = 1 \times 10^{11}\text{cm}^{-2}$ (b) $1 \times 15\text{ n}_{\text{eq}}/\text{cm}^2$; $V_{\text{bias}} = -600\text{V}$; $N_{\text{Ox}} = 1 \times 10^{12}\text{cm}^{-2}$

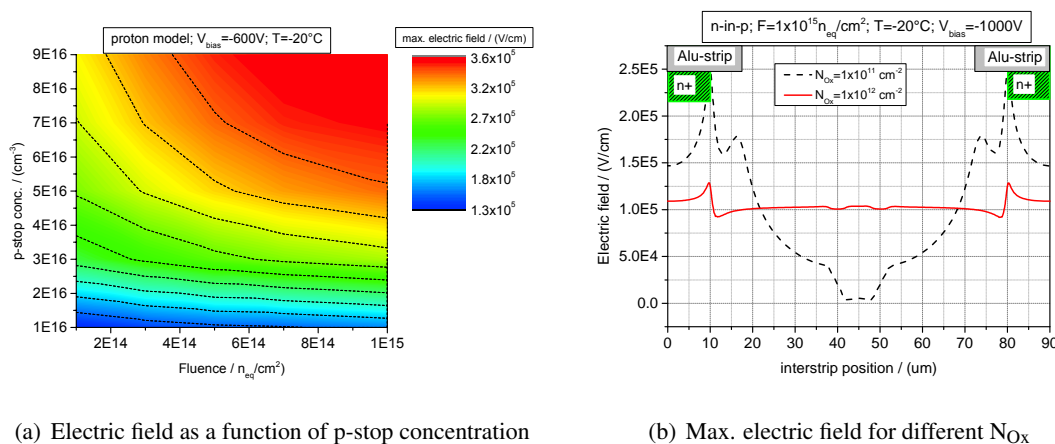
Figure 1. Simulated maximum electric fields of a $300\ \mu\text{m}$ thick sensor with $90\ \mu\text{m}$ pitch and $w/p = 0.22$ depending on the p-stop distance to the center of a neighboring n+ strip and p-stop doping concentration. (a) Unirradiated case performed at $T = 293\text{K}$; (b) Proton irradiation to $1 \times 15\text{ n}_{\text{eq}}/\text{cm}^2$ at $T = 253\text{K}$. The red dashed line in (b) illustrates the critical breakdown field of silicon [8].

3.2 Electric fields and charge collection after irradiation

The different samples have been irradiated with 23 MeV protons at the Karlsruhe Cyclotron [10] and reactor neutrons in Ljubljana [11]. For T-CAD studies the proton model from table 2 was used. In the simulations, one can observe extremely high local electric fields in the bulk near the surface due to high space charge and high bias voltage of $V_{\text{bias}} = -600\text{V}$. Depending on the peak p-stop concentration, the electric fields are even far in excess of $\sim 3 \times 10^5\text{ V/cm}$ which is the electrical breakdown field strength in silicon. The peak electric fields are located at the floating p-stops. The dependence of the maximum electric field strength is shown in figure 1(b) for a proton irradiation to $F = 1 \times 10^{15}\text{ n}_{\text{eq}}\text{cm}^{-2}$. Like in the unirradiated case, maximum electric fields decrease with distance to n+ implants but not as pronounced. In figure 2, a scan of the maximum electric fields depending on the p-stop doping concentration is shown. The fluence was scanned from $F = 1 \times 10^{14}\text{ n}_{\text{eq}}\text{cm}^{-2}$ to $F = 1 \times 10^{15}\text{ n}_{\text{eq}}\text{cm}^{-2}$. The voltage of $V = -600\text{V}$ was chosen as this is the minimum bias voltage in order to deplete a highly irradiated $\sim 300\ \mu\text{m}$ thick silicon bulk, and a constant oxide charge of $N_{\text{Ox}} = 1 \times 10^{12}\text{cm}^{-2}$ was applied.

The p-stop doping concentrations of samples #1 ($\ll 1 \times 10^{16}\text{cm}^{-3}$) have not been covered in the simulations as measurements indicate a far too low interstrip resistance. This results in a smearing of the signal over several strips. Referring to figure 2 the samples #2 with a concentration of boron in the p-stop implants of about $1 \times 10^{16}\text{cm}^{-3}$ and a distance of $25\ \mu\text{m}$ between strip implant edge and p-stop edge seem to feature the lowest electrical field strength and as a consequence probably the most stable operation. The measurements resulted in an interstrip resistance above tens of MOhm what is sufficient for good strip isolation [12]. Increasing oxide charge due to penetration with charged particles or photons is beneficial for the breakdown behavior as higher oxide charge lowers the electric fields in n-in-p type sensors as shown in figure 2b.

All samples have been irradiated to the expected fluence of the HL-LHC era with a 50% safety margin. The charge collection of all samples depending on the p-stop concentration and one exemplary noise histogram from a pedestal run of sample #3 are presented in figure 3.



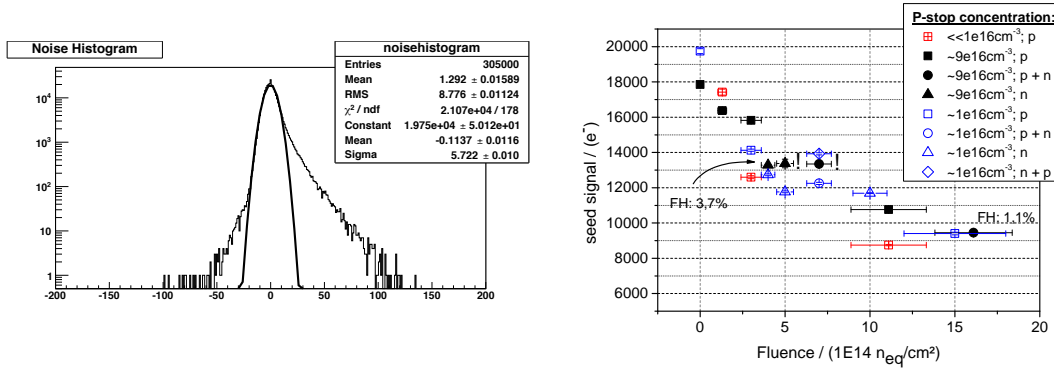
(a) Electric field as a function of p-stop concentration

(b) Max. electric field for different N_{Ox}

Figure 2. Simulated maximum electric fields. $T = 253\text{ K}$ and $V_{\text{Bias}} = -600\text{ V}$. Oxide charge was fixed in (a) to $N_{Ox} = 1 \times 10^{12}\text{ cm}^{-2}$ and the p-stop geometry corresponds to sample #3. In (b), the fluence was fixed to $F = 1 \times 10^{15}\text{ n}_{\text{eq}}\text{ cm}^{-2}$ while the oxide charge was increased from $N_{Ox} = 1 \times 10^{11}\text{ cm}^{-2}$ to $N_{Ox} = 1 \times 10^{12}\text{ cm}^{-2}$. The distance of the p-stop to the edge of the n+ implant was in both cases $25\text{ }\mu\text{m}$.

The results for samples #2 have been obtained from a large measurement campaign, where both sensor polarities have been studied in detail. In this measurement campaign, the n-in-p sensors were isolated either by a p-spray layer or by the p-stop atoll pattern with an approximate peak doping concentration of $1 \times 10^{16}\text{ cm}^{-3}$ which corresponds to the samples #2 in this paper. A non-gaussian noise in pedestal runs of p-in-n sensors has been observed while the n-in-p type sensors did not show any non-gaussian noise at all. The appearance depends on the applied voltage, the particle type and annealing and is described in [13]. Wrong hit identification from non-gaussian noise (fake hits) has been defined as the number of entries exceeding a 5 sigma gaussian noise during a pedestal run divided by the number of strips.

Samples #3 presented in this paper with a comparably high p-stop doping concentration of about $9 \times 10^{16}\text{ cm}^{-3}$ also feature the non-gaussian noise, especially after neutron or mixed irradiation, see figure 3(a). The figure shows that entries with more than 28.5 ADC counts are identified wrongly as hits as the sigma of the noise is 5.7 ADC. The most probable value (MPV) of a convoluted landau-gauss function fitted to the seed signal distribution of the different samples after proton (p), neutron (n) and mixed (n+p, p+n) irradiation is plotted in figure 3(b). The red points of samples #1 with very low p-stop doping concentration are also added for completeness. Samples with $\geq 1\%$ fake hit rate have been labeled with FH:percentage. Clearly, only samples #3 with high p-stop peak doping concentration and neutron or mixed irradiation show fake hits. The simulation results in figure 2 show very high local electric fields for high p-stop concentrations where local avalanche effects can occur. As a consequence from simulation studies and measurements, p-stop doping concentrations and doping depths should be carefully calculated in order to keep the maximum electric fields of n-in-p type sensors as low as possible. On the other side the lower limit of the p-stop concentration must be high enough in order to assure good strip isolation before and after irradiation. Simulations indicate that the value of about $1 - 3 \times 10^{16}\text{ cm}^{-3}$ for the boron concentration in p-stop implants ensures reasonable electric field strengths. Furthermore, first simulation studies with Sentaurus T-CAD and the Silvaco software package have been performed [14, 15]



(a) Histogramm of non-gaussian noise from a pedestal run. (b) Seed signal for three different p-stop concentrations; $F = 7 \times 10^{14} \text{ n}_{\text{eq}} \text{ cm}^{-2}$ (p+n). p indicates proton and n neutron irradiation

Figure 3. Exemplary noise histogram of samples #3 and MPV seed signals of all three samples with different p-stop concentrations measured at $T = 253 \text{ K}$ and $V_{\text{Bias}} = -600 \text{ V}$ with a Sr_{90} source.

where the interstrip capacitance and interstrip resistance have been successfully reproduced and a value of $1 - 3 \times 10^{16} \text{ cm}^{-3}$ ensures good strip isolation before and after irradiation. Accordingly, the p-stop doping concentration for high fluence in the CMS Detector after the Phase II Upgrade can further be optimized using T-CAD tools.

4 Conclusions and outlook

T-CAD studies and Sr_{90} measurements have been performed in order to optimize the p-stop doping concentration for n-in-p type detectors for very high fluence. Samples with different peak concentrations and slightly varying doping depths have been studied with Sentaurus T-CAD. Simulations indicate a strong influence of the p-stop concentration and pattern on the electric field and affinity for microdischarges or local avalanche effects. In sensors with higher p-stop doping concentrations than $4 \times 10^{16} \text{ cm}^{-3}$ and $\sim 2 \mu\text{m}$ depth, electric fields higher than $\sim 3 \times 10^5 \text{ V/cm}$ can occur and negatively affect the sensor performance. Samples with $9 \times 10^{16} \text{ cm}^{-3}$ peak p-stop doping concentration have been produced. They show sufficient interstrip resistance but also misidentified hits. Both simulations and measurements indicate, that the p-stop doping concentration of $9 \times 10^{16} \text{ cm}^{-3}$ is too high and results in high electric field strength. The lower limit for p-stops still has to be identified as meaningful measurements are missing.

Further T-CAD studies and developments of damage models are ongoing in order to predict the sensor performance after high irradiation. Currently, a new batch of sensors is being produced with a fourth vendor where again the p-stop pattern is varied. For each pattern there will be three different peak doping concentrations of $5 \times 10^{15} \text{ cm}^{-3}$, $1 \times 10^{16} \text{ cm}^{-3}$ and $1 \times 10^{17} \text{ cm}^{-3}$. Furthermore two different p-stop doping depths of about $1.5 \mu\text{m}$ and $2.5 \mu\text{m}$ will be realized. The study presented in this paper and the variations from the new batch with further simulations will be taken to identify the optimal isolation parameters for high radiation environment during the HL-LHC era.

Acknowledgments

The research leading to these results has received funding from the European Commission under the FP7 Research Infrastructures project AIDA, grant agreement no. 262025 and was supported by the Initiative and Network Fund of the Helmholtz Association, contract HA-101 (“Physics at the Terascale”).

References

- [1] G. Casse et al., *First results on the charge collection properties of segmented detectors made with p-type bulk silicon*, *Nucl. Instrum. Meth. A* **487** (2002) 465.
- [2] I. Mandic et al., *Observation of full charge collection efficiency in heavily irradiated n+p strip detectors irradiated up to $3 \times 10^{15} n_{eq}/cm^2$* , *Nucl. Instrum. Meth. A* **612** (2010) 474.
- [3] A. Dierlamm, *Planar sensors for future vertex and tracking detectors*, *PoS(Vertex2013)* 027.
- [4] J. Zhang et al., *X-ray induced radiation damage in segmented p+n silicon sensors*, *PoS(Vertex2012)* 019.
- [5] G. Pellegrini et al., *Technology development of p-type microstrip detectors with radiation hard p-spray isolation*, *Nucl. Instrum. Meth. A* **566** (2006) 360.
- [6] M. Valentan et al., *Optimization of strip isolation for silicon sensors*, *Nucl. Instrum. Meth. A* **37** (2012) 891.
- [7] R. Eber, *Investigations of new Sensor Designs and Development of an effective Radiation Damage Model for the Simulation of highly irradiated Silicon Particle Detectors*, Ph.D. Thesis, Karlsruhe Institute of Technology, Karlsruhe Germany (2013), IEKP-KA/2013-27, <http://ekp-invenio.physik.uni-karlsruhe.de/record/48328/files/EKP-2014-00012.pdf>.
- [8] O. Leistiko Jr. and A.S. Grove, *Breakdown voltage of planar silicon junctions*, *Solid State Electron.* **9** (1966) 847.
- [9] R. Marco-Hernandez, *A portable readout system for microstrip silicon sensors (ALIBAVA)*, *IEEE Nucl. Sci. Symp. Conf. Rec.* **2008** (2008) 3201.
- [10] ZAG Zyklotron AG, Irradiation centre, Karlsruhe, Germany, <http://www.zyklotron-ag.de/en/>.
- [11] L. Snoj, G. Žerovnik and A. Trkov, *Computational analysis of irradiation facilities at the JSI TRIGA reactor*, *Appl. Radiat. Isot.* **70** (2012) 483.
- [12] K.-H. Hoffmann, *Development of new Sensor Designs and Investigations on Radiation Hard Silicon Strip Sensors for CMS at the Large Hadron Collider during the High Luminosity Phase*, Ph.D. Thesis, Karlsruhe Institute of Technology, Karlsruhe Germany (2013), IEKP-KA/2013-1, <http://www-ekp.physik.uni-karlsruhe.de/~thesis/data/iekp-ka2013-1.pdf>.
- [13] M. Printz, *Radiation hard sensor materials for the CMS Tracker Phase II Upgrade - Charge collection of different bulk polarities*, *Nucl. Instr. Meth. A* (2014), in press.
- [14] R. Dalal et al., *Development of Radiation Damage Models for Irradiated Silicon Sensors Using TCAD Tools*, *Proceedings of Technology and Instrumentation in Particle Physics 2014*, Amsterdam, the Netherlands, 2–6 June 2014, to be published in JINST, [CMS-CR-2014-120](#) (2014).
- [15] T. Eichhorn et al., *Simulations of Inter-Strip Capacitance and Resistance for the Design of the CMS Tracker Upgrade*, *Proceedings of Technology and Instrumentation in Particle Physics 2014*, Amsterdam, the Netherlands, 2–6 June 2014, to be published in JINST, [CMS-CR-2014-126](#) (2014).